Journal of Sound and Vibration (1998) **210**(1), 117–135

NON-STATIONARY RESPONSE OF A VARIABLE SECTION FLEXIBLE WING AIRCRAFT OVER UNEVEN ELASTIC TRACK

D. Yadav, S. Kamle and S. Talukdar

Department of Aerospace Engineering, Indian Institute of Technology, Kanpur 208016, *India*

(*Received* 24 *July* 1996, *and in final form* 3 *September* 1997)

The coupled dynamics of flexible vehicle-track systems has been analysed with an aircraft in ground runs. The aircraft is modelled as a combination of lumped and continuous members with the wings idealised as variable section beams. The track is treated as a beam resting on an elastic subgrade. Suspension behaviour is assumed to be linear and the track unevenness a non-homogeneous random process. Closed form expressions for second order response statistics have been developed for a general description of vehicle forward motion.

1. INTRODUCTION

Ground vehicles and aircraft during ground manoeuvers receive dynamic excitation from an uneven track. The vibration environment causes fatigue in the vehicle structure, discomfort to passengers and crews, undesirable movement and damage to the cargo and wear and tear to the track. In extreme cases, it may even affect the controllability of the vehicle. Aircraft landing touch-down induces an impact force on the vehicle structure as well as the runway which may be significant for the design of some structural components and the track.

The study of track-induced vehicle dynamics started with simple problems of linear models on pavements with discreet flaws [1]. Subsequently more realistic modelling and efficient solution techniques followed. Linear vehicle models on runways with homogeneous random profile have been analysed at uniform [2–4] and variable [5, 6] velocities. The coupled vehicle-track dynamics have been studied at constant and accelerating vehicle forward motion patterns [7–11].

Many vehicles have slender attachments; aircraft wings may be quoted as an example. These also carry concentrated masses such as fuel tanks, engines, pylons, guns, missiles, bombs, etc. Slender members undergo appreciable deformations under load, and modelling these as rigid may lead to error in estimation of the response. Incorporating the flexibility effects in the vehicle and track model would increase the accuracy of the analysis. In the present paper, a procedure for the analysis of coupled vehicle–track dynamics with elastic appendages has been presented, utilizing a recently proposed approach [12] of analysis for variable section beams. The vehicle considered is an aircraft with flexible wings that carry concentrated mass loadings and distributed damping. Most ground vehicles with slender attachments would fit a similar structural description. The elastic track is assumed to have a non-homogeneous random profile. The vehicle forward velocity may have any general pattern. The system equations of motion have been discretized and decoupled using the

0022–460X/98/060117 + 19 $25.00/0/sv971295

modal approach. Closed form expressions for the second order response statistics have been developed. Numerical results are presented for an aircraft in ground runs.

2. PROBLEM FORMULATION

2.1. MODEL DESCRIPTION

A model of the aircraft and the runway track is shown in Figure 1. The wheel track contact is assumed to be at one point only. The aircraft fuselage is modelled as a rigid lumped sprung mass M_s on to which are attached flexible left and right wings, designated by superscript/subscript L and R respectively (Figure 1a). Each wing is considered to be a cantilever beam having distributed mass m_w, flexural rigidity $E_w I_w$ and damping c_w, that are variable along the span. Various stores carried by the wings are modelled as concentrated mass loadings $M_1, M_2, \ldots, M_p$ located at $s_1, s_2, \ldots, s_p$ from the wing root. The landing gear assembly is idealised as a lumped unsprung mass M_{us}. Linear airspring K_s and viscous damping C_s have been assumed for the aircraft suspension. The tyre stiffness K_{us} and damping C_{us} are also assumed to be linear.

The track pavement has an uneven profile denoted as $h(x)$ above a horizontal datum (Figure 1b). The runway track elastic behaviour is accounted for by modelling the pavement as a Euler–Bernouli beam (Figure 1c), with distributed flexural rigidity $E_p I_p$ and mass m_p, taken constant along the span. The track is supported over elastic subgrade foundation having distributed stiffness k_f and damping c_f, assumed constant.

The system displacements are considered only in the vertical plane (Figure 1). The displacements z_1 and z_2 of the sprung and the unsprung masses are measured from their respective static equilibrium positions. The transverse displacements of both left and right wing w_L and w_R are measured off their respective bending axes drawn from the wing roots. Deflection of the track mean line y is taken transverse to its longitudinal axis-x.

The suspension system, wheel and foundation dampings are general in nature. However, the wing damping is assumed to be proportional to its mass distribution. This is necessitated because of limitation of the decoupling technique for the variable section beams [12].

2.2. VEHICLE FORWARD MOTION

The position of the vehicle at any instant t from a fixed reference point can be described by a polynomial of degree m as

$$x_c(t) = \sum_{k=0}^{m} a_k t^k. \tag{1}$$

This form can be used to represent different conditions of vehicle forward motions with suitable selection of the coefficients.

2.3. TRACK PROFILE

The vertical level $h(x)$ of the track above a flat datum is a non-homogeneous random process with $\Phi_{h_R h_R}(\Omega_1, \Omega_2)$ as its generalised PSD function. The variable mean track level is assumed as a polynomial

$$h_m(x) = \sum_{i=1}^{\ell} h_i x^i. \tag{2}$$

Different mean shapes can be represented with this form.

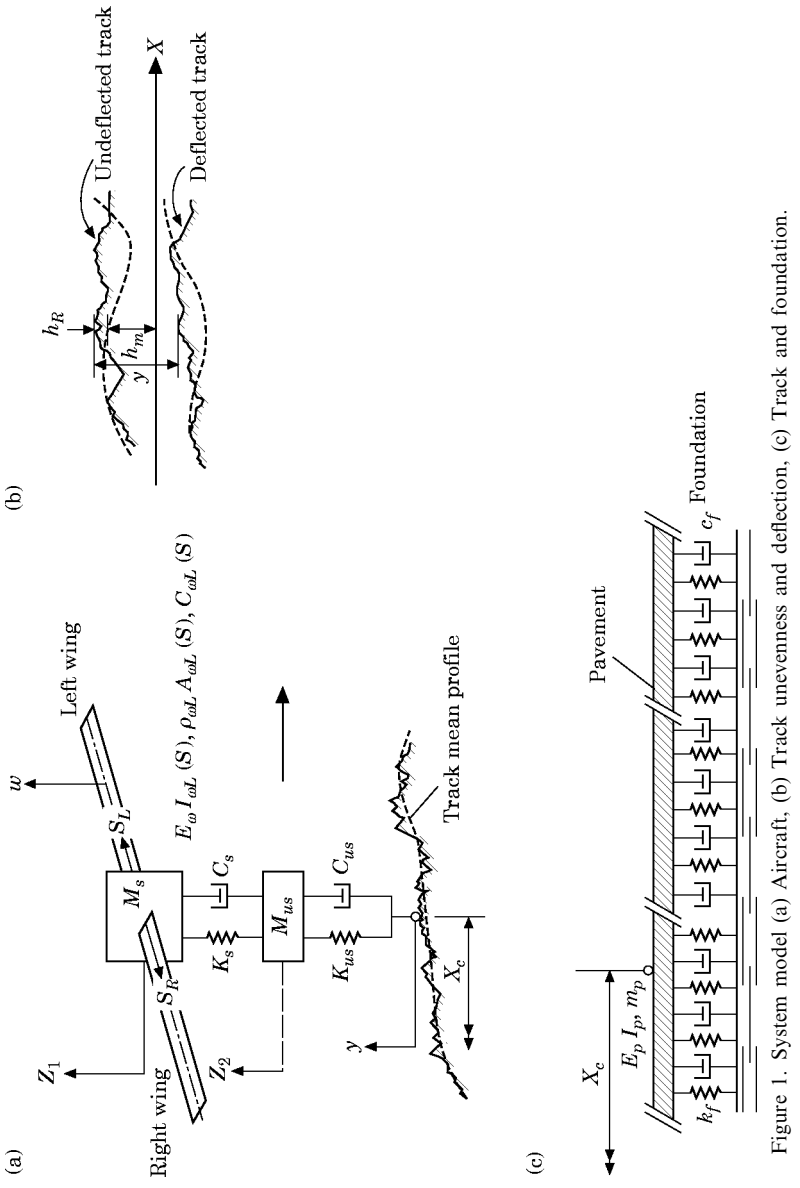

Figure 1. System model (a) Aircraft, (b) Track unevenness and deflection, (c) Track and foundation.

During variable velocity runs the vehicle senses the track input as a time function. Mapping of the temporal frequency ω into the wave number Ω gives [10]

$$\Phi_{h_R h_R}(\Omega_1, \Omega_2) = \Phi_{h_R h_R}(\omega_1 / V_1, \omega_2 / V_2), \tag{3}$$

where V_1 and V_2 are vehicle forward velocities at instants t_1 and t_2 respectively.

Making use of equation (1) in equation (2), the mean track height experienced by the vehicle wheel at instant t may be expressed as [13],

$$h_m(t) = \sum_{i=0}^{\ell} h_i \sum_{r=0}^{mxi} c_{i,r}\, t^r, \tag{4}$$

where $c_{i,0} = a_0^i$, and

$$c_{i,r} = \frac{1}{r a_0} \sum_{k=1}^{r} (ki - r + k) a_k\, c_{i,r-k}, \qquad r \geqslant 1, \qquad (i = 0, 1, \ldots, \ell). \tag{5}$$

2.4. SYSTEM EQUATIONS

The equations of motion of the two lumped masses are

$$M_s \ddot{z}_1 + C_s(\dot{z}_1 - \dot{z}_2) + K_s(z_1 - z_2) = -\frac{\partial^2}{\partial s_L^2}[E_{wL} I_{wL}(s_L)\, \partial^2 w_L / \partial s_L^2]_{S_L = 0}$$
$$- (\partial^2 / \partial s_R^2)[E_{wR} I_{wR}(s_R)\, \partial^2 w_R / \partial s_R^2]_{S_R = 0}, \tag{6}$$

$$M_{us} \ddot{z}_2 + C_{us}\{\dot{z}_2 - \dot{y}(x_c, t) - \dot{h}(x_c)\} + K_{us}\{z_2 - y(x_c, t) - h(x_c)\}$$
$$- C_s(\dot{z}_1 - \dot{z}_2) - K_s(z_1 - z_2) = 0. \tag{7}$$

The wings act like cantilever beams with base excitation as these are clamped at the fuselage and are excited by the fuselage vertical displacements. The distributed aerodynamic lift as well as concentrated mass loadings act on the wing. The equation of motion of the left wing is

$$\frac{\partial^2}{\partial s^2}\left[E_{wL} I_{wL}(s_L) \frac{\partial^2 w_L}{\partial s^2}\right] + m_{wL}(s_L) \frac{\partial^2 w_L}{\partial t^2} + c_{wL}(s_L) \frac{\partial w_L}{\partial t}$$
$$= -\sum_{k=1}^{p_L} M_k^L \frac{\partial^2 w_L}{\partial t^2} \delta(s_L - s_k^L) - \{m_{wL}(s_L)\ddot{z}_1 + c_{wL}(s_L)\dot{z}_1\} + V_L(s_L, t). \tag{8}$$

The equation of motion for the right wing is obtained by exchanging the extension L with R in the above equation. The aerodynamic lift force on either wing can be expressed as [14]

$$V(s, t) = L_0\, V(t)^2 [1 - (s/L_w)]^{1/2}, \qquad \text{where} \quad L_0 = \rho_a\, c_L\, S_w / 2\pi L_w \tag{9}$$

in which ρ_a is the air density, c_L is the lift coefficient, S_w is the wing surface area, L_w is the semiwing span and $V(t)$ is the aircraft forward velocity. For vehicles where aerodynamic lift is not significant, the lift terms may be dropped from equation (8).

The track is assumed to behave like a beam with continuous elastic support along its length. Its differential equation of motion for a single point input is given by [10]

$$E_p I_p \frac{\partial^4 y}{\partial x^4} + m_p \frac{\partial^2 y}{\partial t^2} + c_f \frac{\partial y}{\partial t} + k_f y = -[C_{us} \{\dot{z}_2 - \dot{y}(x_c, t) - \dot{h}(x_c)\} + K_{us} \{z_2 - y(x_c, t) - h(x_c)\}]\delta(x - x_c) \tag{10}$$

where the subscript p refers to the track pavement and f to the foundation subgrade.

Equations (6) to (10) constitute the system governing equations and are required to be solved for the response statistics.

2.5. DISCRETIZATION OF THE WING EQUATION OF MOTION

The distributed mass and bending rigidity of the wings vary along its length. Representing these by polynomial functions and assuming the damping to be proportional to the mass distribution one can write

$$E_w I_w (s) = E_w I_w (0) \sum_{i=0}^{\infty} p_i s^i, \qquad m_w (s) = \rho_w A_w (0) \sum_{i=0}^{\infty} q_i s^i, \qquad c_w (s) = c_w (0) \sum_{i=0}^{\infty} q_i s^i, \tag{11}$$

where ρ_w is the density of the wing material, A_w is the cross-sectional area and the quantities $I_w (0)$, $A_w (0)$ and $c_w (0)$ correspond to the reference station.

Considering the wing deflection w as a superimposition of its normal modes with $\eta_i (t)$ as the normal co-ordinates and $\phi_i (s)$ the associated mode shape functions and invoking the orthogonality property of the normal modes, the discretized equations of motion for the left wing beam takes the form [12]

$$\left[\ddot{\eta}_{Li} (t) + \frac{1}{M_i^{gL}} \sum_{r=1}^{p_L} M_r^L \phi_i^L (s_r^L) \sum_{k=1}^{\infty} \phi_k^L (s_r^L) \ddot{\eta}_{Li} (t)\right] + D_L \dot{\eta}_{Li} (t) + \{(\omega_{Li}^2 - \beta_{Li}^2 - D_L \beta_{Li}) - \mathrm{j}\omega_{Li} (2\beta_{Li} + D_L)\}\eta_{Li} (t) = \frac{1}{M_i^{gL}} \int_{L_{wL}} [-\{m_{wL} (s_L)\ddot{z}_1 + c_{wL} (s_L)\dot{z}_1\} + V_L (s_L, t)]\phi_i^L (s_L)\, \mathrm{d}s_L ; \qquad i = 1, 2, \ldots, \tag{12}$$

where $D = c_w (0)/\rho_w A_w (0)$; ω is the damped natural frequency of the wing and β is a factor related to the damping, M_i^{gL} is the left wing generalised mass given by

$$M_i^{gL} = \int_{L_{wL}} m_{wL} (s_L)\phi_i^L (s_L)^2\, \mathrm{d}s_L . \tag{13}$$

The corresponding relation for the right wing is obtained by replacing extension L by R in equation (12).

2.6. DISCRETIZATION OF THE TRACK EQUATION OF MOTION

The track equation of motion, equation (10) can be discretized in terms of the normal co-ordinates η_{pi} [10]

$$\ddot{\eta}_{pi} (t) + B\dot{\eta}_{pi} (t) + \{(\omega_{pi}^2 - \xi_i^2 - B\xi_i) - \mathrm{j}\omega_{pi} (2\xi_i + B)\}\eta_{pi} (t) = -(\psi_i (x_c)/M_i^p) [\{C_{us} (\dot{z}_2 - \dot{y}(x_c, t) - \dot{h}(x_c)\}$$

$$+ \{K_{us}(z_2 - y(x_c, t) - h(x_c)\}], \qquad i = 1, 2, \ldots, \tag{14}$$

where ω_p is the track damped natural frequency, ξ is a factor related to the foundation damping, $\omega_f^2 = k_f/m_p$, $B = c_f/m_p$ and ψ_i is the modal displacement function of the track beam and M_i^p is the generalised mass for the ith mode.

2.7. DECOUPLING OF THE SYSTEM EQUATIONS

The system equations (6), (7), (12) for left and right wings and (14) are coupled second order ordinary differential equations. If only the first n_w and n_p modes for the wings and the track respectively are retained the number of coupled equations is $n = 2 + 2n_w + n_p$. The system equations can be expressed in matrix notation

$$\mathbf{M}\ddot{\mathbf{q}}(t) + \mathbf{C}\dot{\mathbf{q}}(t) + \mathbf{K}\mathbf{q}(t) = \mathbf{F}(t), \tag{15}$$

where $\mathbf{q}(t)$ is the response vector, $\mathbf{F}(t)$ is the generalised force vector and $\mathbf{M}$, $\mathbf{C}$, and $\mathbf{K}$ are system mass, damping and stiffness matrices respectively.

The system equations (15) can be cast into a $2n$ dimensional first order equation of the following form

$$\dot{\mathbf{p}}(t) + \mathbf{A}\mathbf{p}(t) = \mathbf{P}(t), \tag{16}$$

where

$$\mathbf{p}(t) = \begin{Bmatrix} \dot{\mathbf{q}}(t) \\ \mathbf{q}(t) \end{Bmatrix}, \qquad \mathbf{P}(t) = \begin{Bmatrix} \mathbf{M}^{-1}\mathbf{F}(t) \\ \mathbf{0} \end{Bmatrix}, \qquad \mathbf{A} = \begin{bmatrix} \mathbf{M}^{-1}\mathbf{C} & \mathbf{M}^{-1}\mathbf{K} \\ -\mathbf{I} & \mathbf{0} \end{bmatrix} \tag{17}$$

$\mathbf{I}$ being an identity matrix and $\mathbf{0}$ a null vector/matrix.

It is possible to uncouple the system equations (16) as [15]

$$\dot{v}_i(t) + \alpha_i v_i(t) = R_i(t), \qquad i = 1, 2, \ldots, 2n, \tag{18}$$

with

$$R_i(t) = \sum_{r=1}^{n} \bar{u}_{ir} P_r(t) = \sum_{r=1}^{n} \bar{u}_{ir} \sum_{k=1}^{n} \bar{m}_{rk} F_k, \tag{19}$$

where α_i are the eigenvalues and $\mathbf{u}_i$ the eigenvectors for the matrix $\mathbf{A}$, $\mathbf{v}(t) = \mathbf{U}^{-1}\mathbf{p}(t)$ with $\mathbf{U}$ as the modal matrix, $\bar{u}_{ir}$ and $\bar{m}_{rk}$ as the elements of the inverse of matrices $\mathbf{U}$ and $\mathbf{M}$ respectively.

2.8. RESPONSE STATISTICS

The general solution of equation (18) may be obtained and expressed in terms of the generalised co-ordinates by using equations (17) and (19)

$$q_m(t) = \sum_{i=1}^{2n} X_{oi} u_{m_1 i} \exp(-\alpha_i t)$$

$$+ \sum_{i=1}^{2n} u_{m_1 i} \sum_{r=1}^{n} \bar{u}_{ir} \sum_{k=1}^{n} m_{rk} \int_{-\infty}^{\infty} H_i(\omega, t)\, \mathrm{d}S(F_k(\omega)); \qquad m = 1, 2, \ldots, n, \tag{20}$$

where $m_1 = m + n$, X_{oi} are the constants of integration and $H_i(\omega, t)$ are the transient frequency response functions given by [15]

$$H_i(w, t) = \frac{1}{j\omega + \alpha_i}[\exp(j\omega t) - \exp\{-\alpha_i (t - t_0)\}]. \tag{21}$$

2.8.1. *Mean response*

Expectation of equation (20) yields the mean response

$$\mu_{q_m}(t) = \sum_{i=1}^{2n} X_{oi}\, u_{m_1 i} \exp(-\alpha_i t) + \sum_{i=1}^{2n} u_{m_1 i} \sum_{r=1}^{n} \bar{u}_{ir} \sum_{k=1}^{n} m_{rk}$$

$$\times \int_{-\infty}^{\infty} H_i(\omega, t) \frac{1}{2\pi} \int_{-\infty}^{\infty} \mu_{F_k}(\tau) \exp(-j\omega\tau)\, d\tau\, d\omega, \qquad m = 1, 2, \ldots, n. \tag{22}$$

The mean generalised force μ_F depends on the track profile characteristics as well as the aerodynamic lift force. The kth element of the mean generalised force vector can be expressed as

$$\mu_{F_k}(t) = A_k h_m(t) + B_k \dot{h}_m(t) + C_k V(t)^2, \tag{23}$$

in which the coefficients A_k, B_k and C_k are given by

$$A_k = \begin{cases} 0, & k = 1, 3, 4, \ldots, n_1, \\ K_{us}, & k = 2, \\ (\psi_{k-n_1})/M^p_{k-n_1} K_{us}, & k = n_1 + 1, n_1 + 2, \ldots, n, \end{cases} \tag{24}$$

where $n_1 = 2n_w + 2$.

$$C_k = \begin{cases} 0, & k = 1, 2, n_1 + 1, n_1 + 2, \ldots, n, \\ \dfrac{L_0}{M^{gL}_{k-2}} \displaystyle\int_{L_{wL}} \phi^L_{k-2}(s_L)\,(1 - (s_L/L_{wL}))^{1/2}\, ds_L, & k = 3, 4, \ldots, n_w + 2, \\ \dfrac{L_0}{M^{gR}_{k-2}} \displaystyle\int_{L_{wR}} \phi^R_{k-(n_w+2)}(s_R)\left(1 - \frac{S_R}{L_{wR}}\right)^{1/2} ds_R, & k = (n_w + 3), (n_w + 4), \ldots, n_1. \end{cases} \tag{25}$$

B_k is obtained from equation (24) by replacing K_{us} with C_{us}.

Using equations (21) and (23) in equation (22), and performing the integration over ω, yields

$$\mu_{q_m}(t) = \sum_{i=1}^{2n} X_{oi}\, u_{m_1 i} \exp(-\alpha_i t) + \sum_{i=1}^{2n} u_{m_1 i} \sum_{r=1}^{n} \bar{u}_{ir} \sum_{k=1}^{n} m_{rk} I_{ik}(t); \qquad m = 1, 2, \ldots, n, \tag{26}$$

where

$$I_{ik}(t) = A_k I_1(t) + B_k I_2(t) + C_k I_3(t). \tag{27}$$

The components I_1, I_2 and I_3 are

$$I_1(t) = \left(h_0 + \sum_{i=1}^{\ell} h_i\, c_{i,0}\right) J_1 + \sum_{i=1}^{\ell} h_i \sum_{r=1}^{mxi} c_{i,r}\, J_2, \tag{28}$$

$$I_2(t) = \sum_{i=1}^{\ell} h_i\, c_{i,1}\, J_1 + \sum_{i=1}^{\ell} h_i \sum_{r=1}^{mxi-1} c_{i,r+1}\,(r+1) J_2, \tag{29}$$

$$I_3(t) = c_0'\, J_1 + \sum_{r=1}^{2(m-1)} c_r'\, J_2, \tag{30}$$

with

$$J_1 = (1/\alpha_i)\{1 - \exp(-\alpha_i\, t)\},$$

$$J_2 = \frac{t^r}{\alpha_i} + \sum_{k=1}^{r} \frac{(-1)^k r!}{(r-k)!} \frac{t^{r-k}}{\alpha_i^{k+1}} - (-1)^r \frac{r!}{\alpha_i^{r+1}} \exp(-\alpha_i\, t). \tag{31}$$

Utilizing the set of equations (27)–(31) in equation (26), the mean displacement $\mu_{q_m}(t)$ can be obtained. The mean velocity may be found by substituting u_m for u_{m_1} in the expression for μ_{q_m}. The mean acceleration is determined by differentiating mean velocity with respect to t.

2.8.2. *Covariance response*

Utilizing equations (20) and (22), the expression for the response covariance of the system generalised co-ordinates can be put as

$$K_{q_i q_k}(t_1, t_2) = \sum_{\ell=1}^{2n} \sum_{r=1}^{n} \sum_{p=1}^{2n} \sum_{s=1}^{n} \sum_{b=1}^{n} \sum_{w=1}^{n} u_{i_n \ell}\, \bar{u}_{\ell r}\, \bar{m}_{rs}\, u_{k_n p}\, \bar{u}_{pb}\, \bar{m}_{bw} \{I_{s,b}(t_1, t_2) - I_{\ell s}(t_1) I_{pb}(t_2)\},$$

$$i, k = 1, 2, \ldots, n, \tag{32}$$

where $i_n = i + n$, $k_n = k + n$, $I_{\ell s}$ and I_{pb} are defined in equation (27) and $I_{s,b}$ is given by

$$I_{s,b}(t_1, t_2) = \int_{-\infty}^{\infty} \int_{-\infty}^{\infty} H_\ell(\omega_1, t_1) H_p^*(\omega_2, t_2) \Phi_{F_s F_b}(\omega_1, \omega_2)\, \mathrm{d}\omega_1\, \mathrm{d}\omega_2. \tag{33}$$

Assuming the aerodynamic lift to be uncorrelated to the track roughness, $\Phi_{F_s F_b}(\omega_1, \omega_2)$ can be expressed as,

$$\Phi_{F_s F_b}(\omega_1, \omega_2) = \begin{cases} 0, & s = b = 1, 3, 4, \ldots, n_1, \\ \phi_{F_2 F_2}(\omega_1, \omega_2), & s = b = 2, \\ \dfrac{\psi_{s-n_1}}{M^p_{s-n_1}} \dfrac{\psi_{b-n_1}}{p_{M_{b-n_1}}} \Phi_{F_2 F_2}(\omega_1, \omega_2), & s = b = n_1 + 1, \ldots, n, \end{cases} \tag{34}$$

with

$$\Phi_{F_2 F_2}(\omega_1, \omega_2) = \{C_{us}^2\, \omega_1\, \omega_2 + \mathrm{j} C_{us}\, K_{us}(\omega_1 - \omega_2) + K_{us}^2\} \Phi_{h_R h_R}(\omega_1, \omega_2). \tag{35}$$

To proceed further, the PSD of the track roughness process is required. Numerical results have been obtained with the PSD assumed as in reference [10]

$$\Phi_{h_R h_R}(\Omega_1, \Omega_2) = A_r \exp(-k_r \Omega_1^2)\delta(\Omega_1 - \Omega_2). \tag{36}$$

Integral $I_{s,b}$ for the base value $s = b = 2$ takes the form

$$I_{2,2}(t_1, t_2) = \frac{2\pi A_r V_1}{v_r}\left[\exp\left\{-\frac{\alpha_\ell}{v_r}|v_r t_1 - t_2|\right\} - \exp(-\alpha_\ell t_1 - \alpha_p t_2)\right]\exp\left(\frac{k_r \alpha_\ell^2}{V^2}\right)$$

$$\times\left\{\frac{v_r K_{us} + (1 - v_r)C_{us} K_{us} \alpha_\ell - C_{us} \alpha_\ell}{(\alpha_\ell + v_r \alpha_p)}\right\}, \tag{37}$$

where $v_r = V_1 / V_2$. The integrals for other suffixes can be obtained from equations (34) and (37).

Substituting the value of $I_{s,b}(t_1, t_2)$, the covariance of displacement $K_{q_i q_k}(t_1, t_2)$ is known from equation (32). The velocity covariance is obtained by substituting $u_{i\ell}$ and u_{kp} for $u_{i_1 \ell}$ and $u_{k_1 p}$ respectively in the expression for $K_{q_i q_k}$. The covariance of acceleration has to be obtained by differentiating the velocity covariance successively with respect to t_1 and t_2.

3. RESULTS AND DISCUSSIONS

A passenger plane has been selected for the study. The following system data have been adopted to generate numerical results: sprung mass $(M_s) = 1{\cdot}44 \times 10^5$ kg, unsprung mass $(M_{us}) = 2{\cdot}22 \times 10^3$ kg, linearised stiffness of the landing gear $(K_s) = 29{\cdot}62 \times 10^6$ N/m, tyre stiffness $(K_{us}) = 16{\cdot}92 \times 10^6$ N/m, linearised damping in the landing gear $(C_s) = 103 \times 10^4$ Ns/m, tyre damping $(C_{us}) = 0{\cdot}5 \times 10^4$ Ns/m, wing semi span $(L_w) = 10{\cdot}0$ m, aspect ratio $(A_T) = 7{\cdot}08$, flexural rigidity at root section $(E_w I_w(0)) = 7{\cdot}174 \times 10^6$ Nm^2, mass at the root section $(\rho_w A_w(0)) = 42{\cdot}7$ kg/m, concentrated masses on each wing M_1, $M_2 = 0{\cdot}2\rho_w A_w(0)L_w$ at $s_1 = 0{\cdot}46L_w$ and $s_2 = 0{\cdot}72L_w$, damping at root section $(c_w(0)/\rho_w A_w(0)) = 0{\cdot}16$ s^{-1}, lift coefficient $(C_L) = 0{\cdot}8$, density of air $(\rho_a) = 1{\cdot}20$ kg/m^3, runway length $(L_p) = 1400$ m, track mass $(m_p) = 3620$ kg/m, track flexural rigidity $(E_p I_p) = 1{\cdot}38 \times 10^7$ Nm^2, foundation spring constant $(k_f) = 1{\cdot}7 \times 10^8$ N/m^2, foundation damping $(\xi_f) = 0{\cdot}04$, roughness constant $(A_r) = 0{\cdot}51 \times 10^{-5}$, correlation constant $(k_r) = 0{\cdot}102$. Track mean profile is assumed to be a combination of uniform slope (1 in 1000) and sinusoidal vertical curve of wave length (W_1) 100π m and amplitude (A_0) 0·05 m. The coefficients of the polynomial $h_m(x)$ are $h_1 = (0{\cdot}001 + A_0 2\pi/W_1)$, $h_2 = 0$, $h_3 = -(A_0/3!)(2\pi/W_1)^3$, $h_4 = 0$, $h_5 = (A_0/5!)(2\pi/W_1)^5$ etc.

Response statistics of the aircraft model has been obtained for constant velocity taxi, accelerating takeoff and decelerating landing runs during ground manoeuvers. The responses selected for study are displacements, velocities and accelerations of the sprung mass, unsprung mass and the first three normal co-ordinates for the wing and the track modes. Only the left wing response is presented as the other wing has similar characteristics. The mean and the variance of these are plotted as time histories.

3.1. TAXI RUN

The aircraft is assumed to move forward at constant velocity in the taxi run. The results are presented for three forward velocities—40 km/h, 60 km/h and 80 km/h. The plots are shown for the initial 20 s period.

The mean responses are presented in Figure 2. The response of the sprung and unsprung masses and the track modes are influenced primarily by the mean track profile. Initial

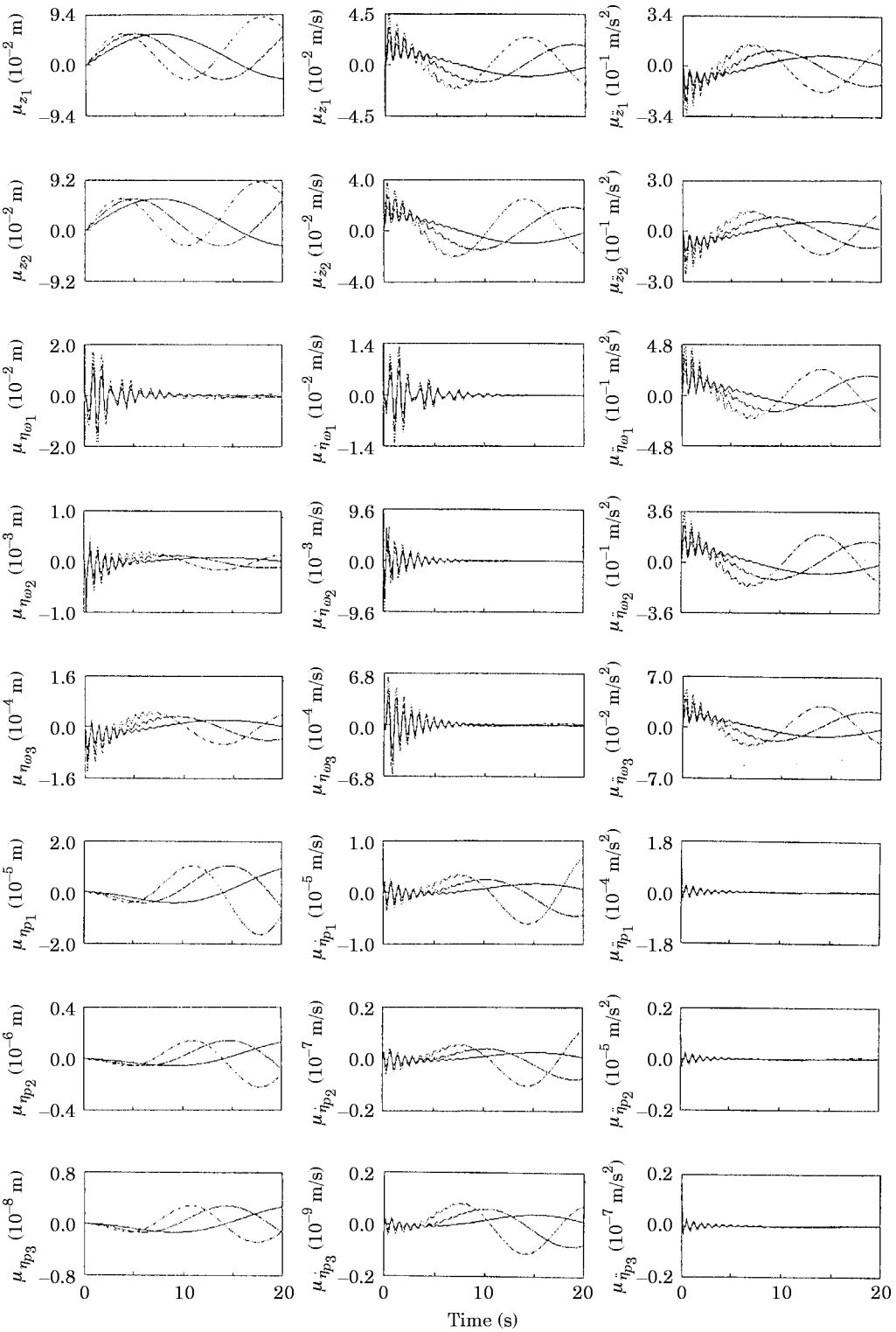

Figure 2. Mean responses for taxi run. Key: vehicle speed (km/h); ——, 40; — - —, 60; · · · · · · · · ·, 80.

transience is small and gets dampened out quickly. The magnitude of these mean displacements, during early phases of travel, does not show much variation with vehicle velocity. However, with the elapse of time, a higher velocity seems to produce increased displacement. The displacement mean response of the wing's first three normal co-ordinates has initial high transient values, diminishing to a steady state oscillation. The mean steady state value is lower compared to the transient response. A higher vehicle velocity is found to produce larger amplitudes for the wing modes. This pattern is followed by the velocity and acceleration response also.

The mean velocities of the lumped masses and the track modes reveal stronger and more persistent transience compared to the displacement response. Except for the wing normal modes, which show very low values, the other steady state velocity responses have the same general pattern as the displacements with a difference in phase. The magnitude of the mean velocity is higher for higher vehicle velocity.

The mean acceleration of the lumped masses follows a pattern somewhat similar to their mean velocity, except for the difference in phase. The wing normal mode mean accelerations have sustained steady state values that are sensitive to the vehicle forward velocity. The mean acceleration of the track's first three normal co-ordinates has initial transience on entry of the vehicle over the track which is quickly dampened out.

The transient mean response shows the presence of a dominant frequency which does not change with forward velocity. This indicates its association with the structural mode, rather than the external excitation. In most of the cases, the vehicle forward velocity is seen to modify the steady state response frequency of oscillation.

The response variances are presented in Figure 3. The displacement variances show that in the early stage, the response is oscillatory with a high peak at the onset of vehicle motion. Subsequently the response subsides to reach a steady asymptotic value. The steady state covariance magnitudes for displacements are higher for higher vehicle speeds. The track mode characteristics have low frequency variations in the steady state. The variances of the velocity response follow a trend similar to the displacements. The acceleration variances indicate dominant values at the initiation of motion. The steady state condition is reached within a shorter time than that for displacement and velocity without any oscillations, showing progressively smaller peaks. The steady state values, however, are very low compared to the initial values.

Increase in the vehicle speed is seen to increase the magnitude of the response variances for all the co-ordinates. Comparison of response mean and variance in the first three flexible wing and track bending modes indicates that response magnitude decreases as the order of mode increases. This conforms to the usual assumption that the lower modes dominate the higher ones.

3.2. TAKEOFF RUN

The aircraft is assumed to start from rest, increasing its speed at uniform accelerations of 1·6 m/s^2, 1·8 m/s^2 and 2·0 m/s^2 to takeoff. The takeoff speed is taken to be 216 km/h. The time history plots are from the start of the aircraft's forward motion until it lifts off.

Figure 4 presents the mean responses. The initial portion of the vehicle response shows low magnitude transience. The accelerating vehicle takes some time to attain a certain level of velocity for the track input to become effective in setting up vibration in the vehicle structure. Subsequently, mean response magnitude grows with increase in vehicle speed and track mean elevation. The influence of the mean track profile is apparent in the vehicle mean response pattern—increasing level with sinusoidal variation. The constant frequency transient oscillation, as in taxi, is not observed in the takeoff run. Mean acceleration

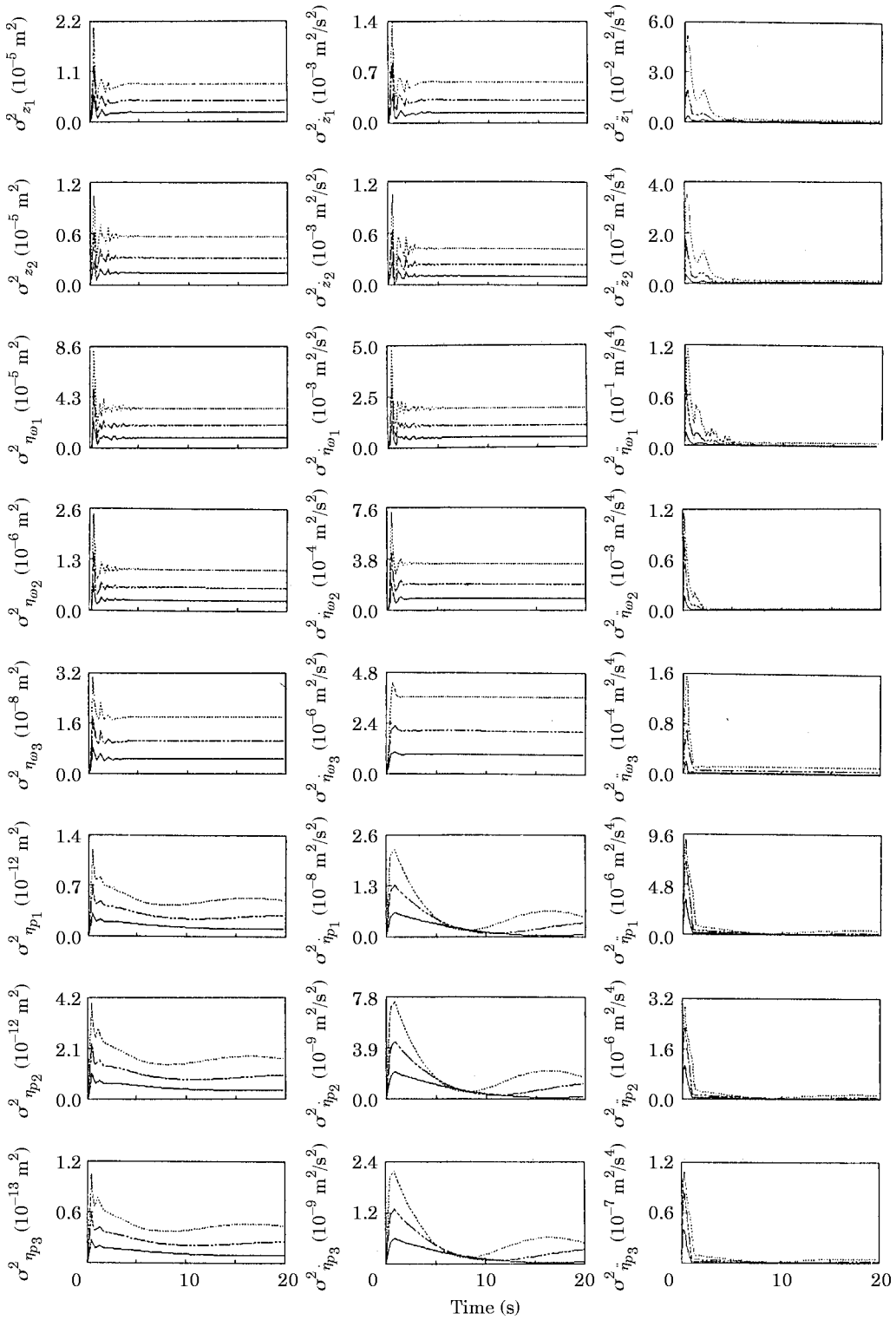

Figure 3. Response variance for taxi run: key as in Figure 2.

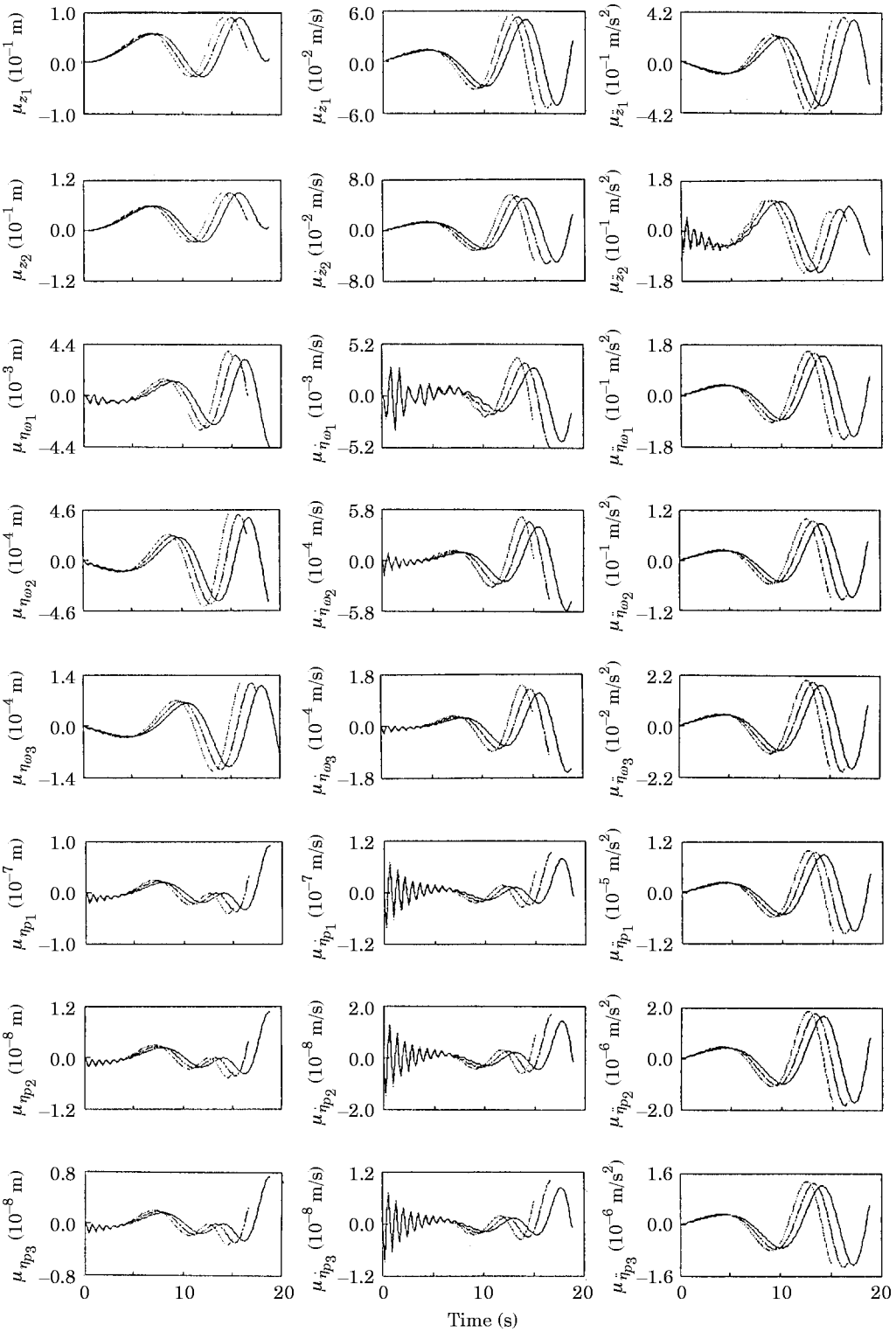

Figure 4. Mean response for takeoff run. Key: vehicle acceleration (m/s^2); ——, 1·6; — - —, 1·8; · · · · · · · · ·, 2·0.

response of unsprung mass starts with high frequency oscillation which finally reaches a steady state pattern.

The magnitude of the mean displacement responses of the track beam is quite low compared to that in constant velocity run. This may be because as the moving load is passing fast over the track beam, the track structure has little time to react to this load. The mean velocity has stronger initial transience and its magnitude is comparable to the steady state values. The mean acceleration of the first three normal co-ordinates of the track has high values prior to takeoff.

The response variances in takeoff run are presented in Figure 5. The variances for the vehicle response show very low values in the initial stage. As the vehicle accelerates from rest, the track input increases in strength with an increase in forward velocity. The variance characteristics of the vehicle also follow this pattern. The magnitude of the variances is seen to increase with the forward acceleration of the vehicle, but at takeoff time the differences in magnitudes are very small. The unsprung mass response variances are smaller when compared to the sprung mass in displacement but larger in velocity and acceleration.

The variances of the first three track normal co-ordinates have an oscillatory pattern about an increasing mean level. There is a gradual increase in amplitude of oscillation until takeoff. Higher vehicle accelerations induce increased response variances of the track's first three normal co-ordinates. The oscillatory trend increases from displacement to velocity to acceleration response.

3.3. LANDING RUN

The time histories are taken from touch down to the stoppage of the forward motion of the aircraft. The results are presented for sink velocities 0·6, 0·9 and 1·2 m/s. The glide velocity and deceleration are assumed to be 215 km/h ad 1·5 m/s^2, respectively in each case. The shock strut at the time of landing, being under no load, is fully extended. The initial displacements of the sprung and unsprung masses are assumed to be their corresponding static values. The initial velocities for them are the sink velocity of the aircraft. The initial condition for the wing relative to the sprung mass and for the track is assumed to be zero. Response characteristics plots have been obtained from the instant of touch down till stoppage of the aircraft's forward motion.

Figure 6 presents the mean displacement response of the vehicle-track system. The response pattern shows initial high values due to touch down impact, increasing with a rise in sink velocity. After the initial impact energy is dissipated, the steady state response becomes dependent on the track roughness. The mean track input frequency is seen to play a dominant role in the steady state displacement response. As the vehicle loses its forward velocity, the effectiveness of input from the track decreases, reducing the system response. The magnitude of responses during the impact phase is larger than that of the taxi and takeoff runs. The mean displacement and velocity of the wing's first normal co-ordinates show the development of the highest peak subsequent to impact. The velocity mean for the wing's second normal co-ordinate indicates the presence of more than one frequency in the oscillation during the impact phase.

Response variances are presented in Figure 7. Strong oscillatory patterns are present for all the displacements and for the vehicle velocity responses in the touch down phase which subsequently decrease gradually with the slowing of the vehicle's forward motion. The magnitude of the first peak seems to be higher with higher sink velocity. The wing's third mode velocity variance rises to a peak after impact and then decreases with a slow rate showing little oscillation. The initial oscillations are not apparent for the velocity variances of track modes. These, however, indicate the presence of oscillation in the steady state

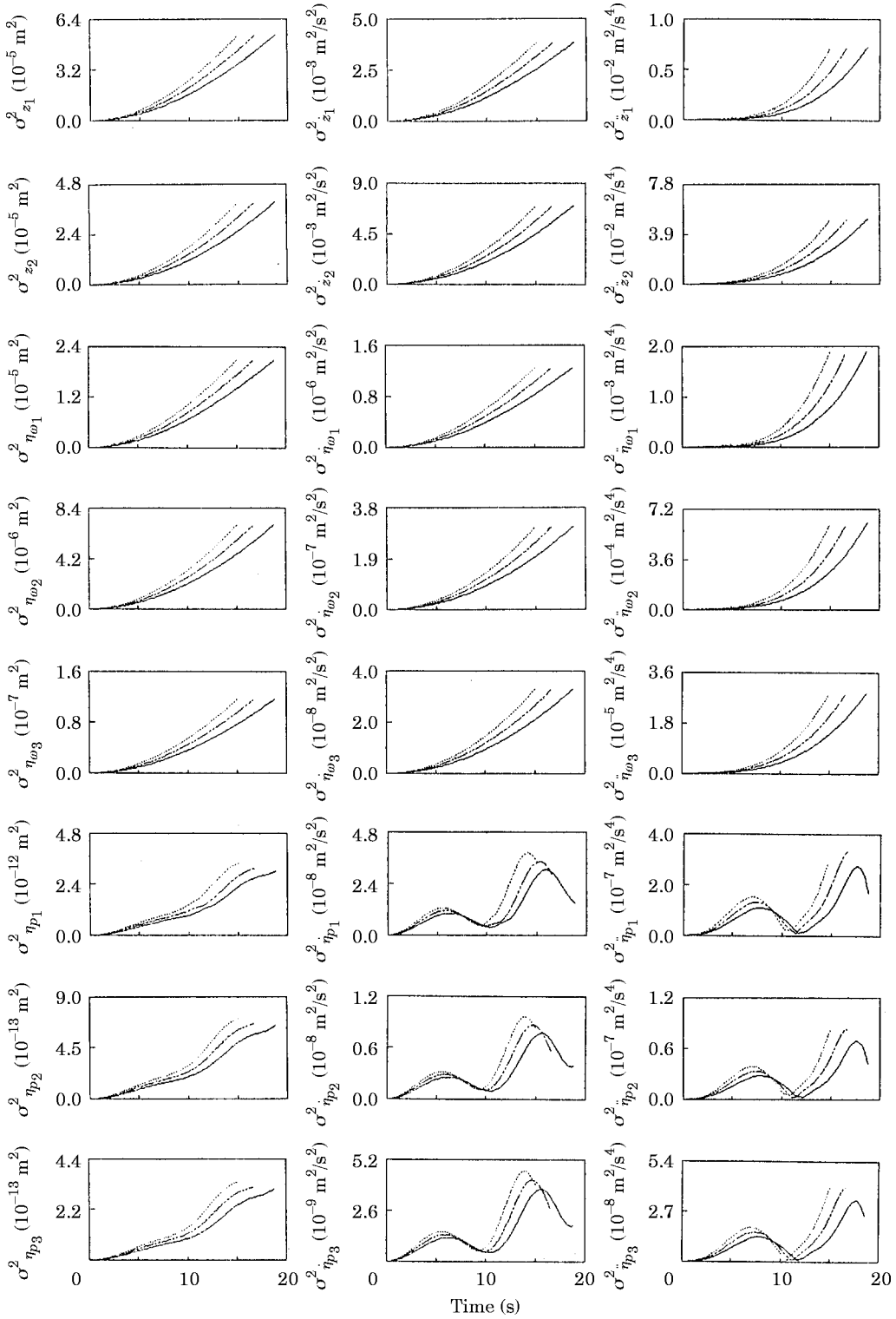

Figure 5. Response variance for take off run: key as in Figure 4.

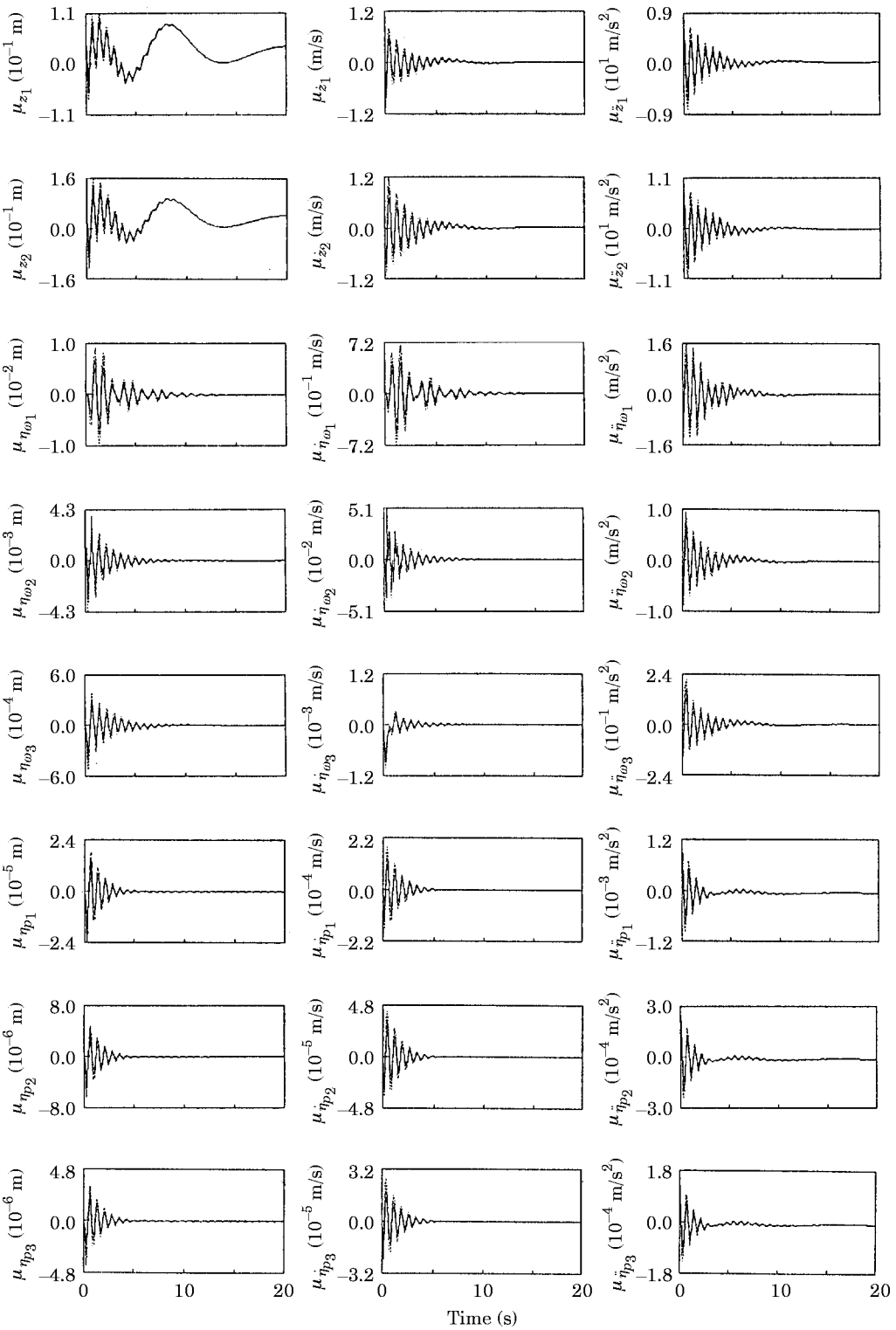

Figure 6. Mean response for landing run. Key: sink velocity (m/s); ——, 0·6; — - - —, 0·9; · · · · · · · · ·, 1·2.

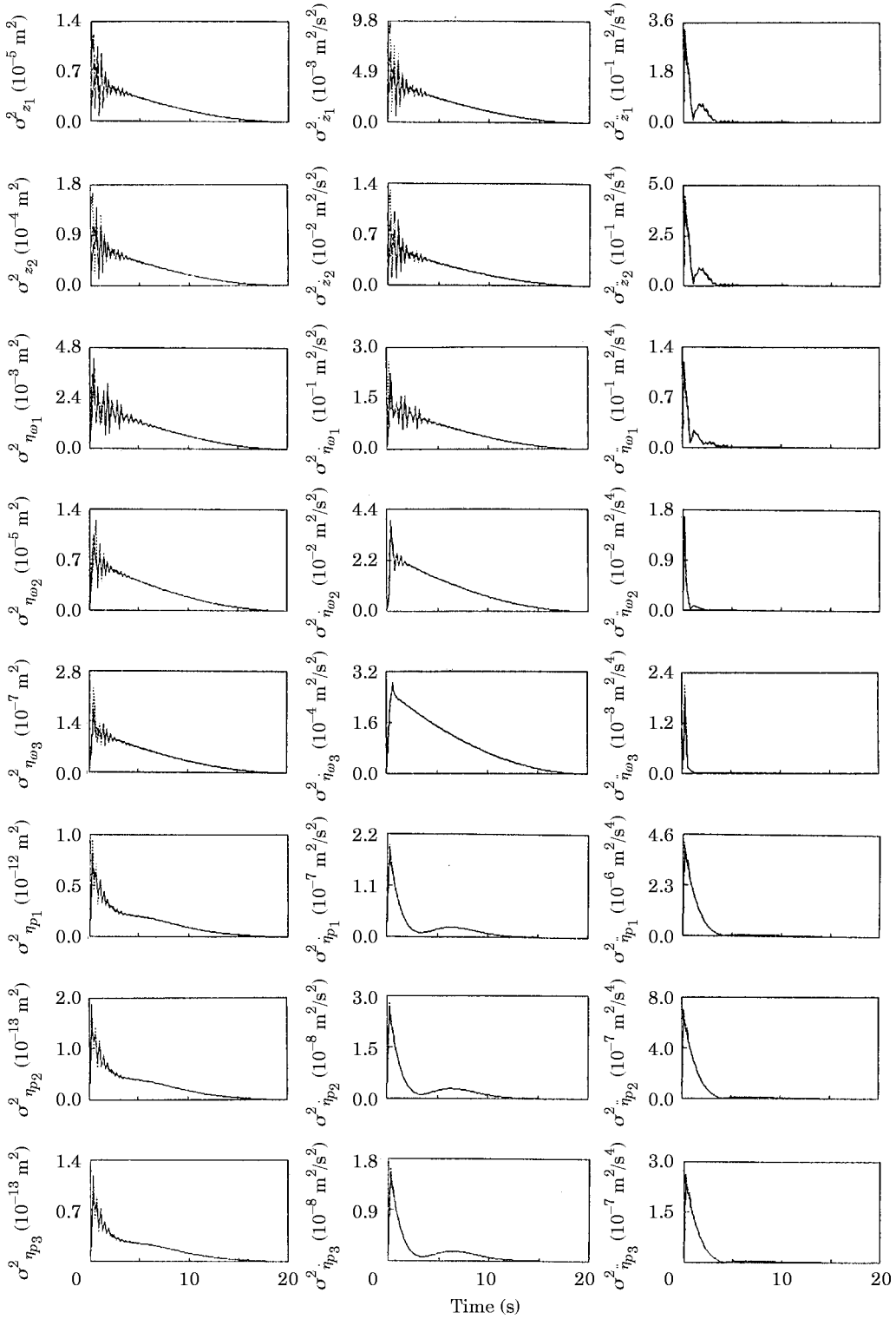

Figure 7. Response variance for landing run: key as in Figure 6.

phase. The initial impact oscillations are subdued in the acceleration variance showing only one or two peaks.

4. CONCLUSIONS

In the present paper an analytical approach to the study of the flexible vehicle–flexible track coupled dynamics has been presented. A vehicle model with lumped masses combined with variable section continuous elements has been used. The method is restricted to linear suspension and tyre model of the vehicle as well as linear track/pavement behaviour. It incorporates any deterministic forward velocity description of the vehicle. Non-homogenity of the track profile characteristics can be handled. Modal analysis used to decouple the system equations allows vehicle suspension and pavement dampings to be general. Any deterministic function describing the mean track profile and any suitable function for the track generalised power spectral density can be used to obtain the second order system response statistics. Some conclusions arrived at in this study with aircraft ground runs are presented below.

Mean response characteristics of the vehicle are dependent on the mean description of the track profile whereas the nature of the covariance response depends on the track profile second order statistics. It is important to maintain the mean level as well as superimposed random unevenness in the track profile low to keep the vehicle–track response level low.

All the responses are higher during the landing impact phase at touch down compared to the taxi and takeoff runs. Flexible wings have strong transients set up at landing touch down, and the response suggests that its inclusion in the rigid aircraft model is important for the analysis of possible metal fatigue damage as well as for catastrophic failure. The flexible wing has appreciable response in the taxi as well as takeoff runs also. Thus, inclusion of slender members in the vehicle model is important for design and performance considerations.

A runway track modelled as a beam responds to vehicle imposed loads in different runs. The response is dependent on vehicle forward velocity and roughness input to the vehicle. The evaluated magnitude of the track deformation is very low for the vehicle parameters, track and subgrade properties in the example selected for this study of a passenger aircraft on a flexible bituminous pavement. This low level of track deformation may not strongly affect the response of the vehicle. However, it may be important for prediction of track fatigue life, maintenance and rehabilitation. For some different combinations of vehicle and track data the pavement response may be significant.

REFERENCES

1. J. C. Houbolt 1961 *Proceedings of the American Society of Civil Engineers*, *Journal of Air Transport Division* **87**, 11–31. Runway roughness studies in the aeronautical field.
2. N. S. Silby 1962 *NASA* **TND-1492.** An analytical study of effects of some airplanes and landing gear factors of the response to runway roughness with application to supersonic aircraft.
3. C. C. Tung, J. Penzien and R. Horonjeff 1964 *NASA* **CR-119**. The effect of runway unevenness on the dynamic response of the supersonic aircraft.
4. C. L. Kirk and P. J. Perry 1971 *Journal of the Royal Aeronautical Society* **75**, 182–194. Analysis of taxiing induced vibration in aircraft by the power spectral density method.
5. K. Sobczyk and D. S. Macvean 1976 *Stochastic Problems on Dynamics*, *University of Southampton* (Editor B. L. Clarkson), 412–434. Non-stationary random vibration of system travelling with variable velocity.
6. R. F. Harrison and J. K. Hammond 1981 *Transactions of the American Society of Mechanical Engineers*, *Dynamic Systems Measurements and Control* **103**, 245–250. Nonstationary response of vehicles on rough grounds—a state space approach.

7. T. E. Blejwas 1979 *Journal of Sound and Vibration* **67**, 513–521. Dynamic interaction of moving vehicles and structures.
8. P. S. Patil 1988 *Journal of Engineering Mechanics*, *American Society of Civil Engineers* **114**, 688–703. Response of infinite rail road track to vibrating mass.
9. D. G. Duff 1990 *Transactions of the American Society of Mechanical Engineers*, *Journal of Applied Mechanics* **57**, 66–73. The response of an infinite rail road track to moving, vibrating mass.
10. D. Yadav and H. C. Upadhyay 1991 *Journal of Sound and Vibration* **147**, 57–71. Non-stationary dynamics of train and flexible track over inertial foundation during variable velocity runs.
11. Y. Cai, S. S. Chen, D. M. Rote and H. T. Coffey 1994 *Journal of Sound and Vibration* **175**, 625–646. Vehicle/guide way interaction for high speed vehicles on a flexible guide way.
12. D. Yadav, S. Kamle and S. Talukdar 1997 *Journal of Sound and Vibration* (to be published). Transverse vibration of multimass loaded variable section beams under random excitation.
13. I. S. Gradshteyn and I. M. Rhzhik 1980 *Tables of Integral*, *Series and Products*. New York: Academic Press.
14. R. C. Shevell 1989 *Fundamentals of Flight*. New Jersey: Prentice Hall.
15. N. C. Nigam 1983 *Introduction to Random Vibration*. Cambridge, MA.: MIT Press.